

Control of multiple non-holonomic air vehicles under wind uncertainty using model predictive control and decentralized navigation functions

Giannis P. Roussos, Georgios Chaloulos, Kostas J. Kyriakopoulos, John Lygeros

Abstract—We present a novel control scheme for multiple non-holonomic vehicles under uncertainty, which can guarantee collision avoidance while complying with constraints imposed on the vehicles. *Dipolar Navigation Functions* are used for decentralized conflict-free control, while Model Predictive Control is used in a centralized manner in order to ensure that the resulting trajectories remain feasible with respect to the constraints present and to optimize the performance objectives. The model used is chosen to resemble air traffic control problems, with some uncertainty introduced in the system. The efficiency of the control strategy is demonstrated by realistic simulations.

I. INTRODUCTION

Navigation Functions (NF), introduced by Rimon and Koditschek [1] as an improved potential field method, have been used so far in a variety of problems, mainly in the robotics field, for the control of single or multiple mobile vehicles. The main advantage of Navigation Functions, compared to most potential field methods, is the lack of any local minima, which are a significant drawback of many potential field methods. Control based on NFs offers a number of benefits, most importantly it can provide provable convergence to the desired configuration, as well as guaranteed collision avoidance.

In its original form the NF methodology addressed problems involving a single robot and a number of stationary obstacles. Following Rimon and Koditschek’s work, the original framework has been extended to multiagent-multirobot systems, both in centralized [2] and decentralized schemes [3], as well as non-holonomic vehicles in single agent [4] and multiagent [5] problems. In addition applications include formation control [6], while lately an extension to 3-dimensional problems has been proposed [7].

While the NF methodology features appealing characteristics as mentioned above, it does not take into account the constraints present in many real applications. Such constraints can be imposed in the form of bounded velocity, smoothness requirement for the path, time constraints etc. In order to overcome this problem we employ the technique of Model Predictive Control (MPC) [8], a control methodology developed specifically to deal with state and input constraints. MPC is used in a level above NF in order to ensure that

the resulting trajectory will be feasible with respect to the constraints present. The resulting control strategy is a novel combination of NFs as a lower level controller and MPC as a higher level, overseeing controller that offers the best of both worlds: safety is guaranteed by NFs, while constraint satisfaction is handled by MPC.

We apply this control technique to problems of conflict¹ avoidance in Air Traffic Control (ATC). ATC is an area where the guaranteed safety that NFs can offer is very valuable for Conflict Detection and Resolution (CD&R) algorithms [9], but the lack of any provision for handling constraints has been a major disadvantage. The proposed control scheme can deal with this drawback of the NF method. In addition we introduce some uncertainty in the problem to account for the effect of the wind on the motion of aircraft. We should note the great resemblance of the proposed scheme to the structure of an ATC situation, where aircraft are navigating in a self-separation airspace (agents navigating with the use of NFs), assisted by a ground tool that seeks to optimize longer term goals (MPC). These are what is known as Short-Term and Mid-Term CD&R algorithms; a thorough overview and classification of the literature in this area can be found in [10].

The rest of the paper is organized as follows: Section II describes the NF method used along with the vehicles’ model, followed by Section III where MPC is briefly introduced and the control scheme outlined above is presented. Simulation results for typical ATC scenarios are presented in Section IV. Finally, conclusions and directions for possible extensions are presented in Section V.

II. NAVIGATION FUNCTION CONTROL

A. Introduction

A Navigation Function produces a potential field whose negated gradient drives the vehicle toward the destination and away from any obstacles present in the workspace. In contrast to other artificial potential fields, Navigation Functions have exactly one minimum and can provide almost global navigation to the goal position and away from obstacles. As Koditschek and Rimon have demonstrated [11], strict global navigation is not possible as every obstacle introduces at least one saddle point in the potential field, nevertheless the sets of initial conditions that drive the system to these saddle points are of measure zero.

Giannis P. Roussos and Kostas J. Kyriakopoulos are with the Control Systems Lab, Department of Mechanical Engineering, National Technical University of Athens, 9 Heron Polytechniou Street, Zografou 15780, Greece. email: {jrous, kkyria}@mail.ntua.gr

Georgios Chaloulos and John Lygeros are with the Automatic Control Laboratory, Department of Electrical Engineering, Swiss Federal Institute of Technology (ETH), Physikstrasse 3, ETL I28, 8092, Zürich, Switzerland. email: {chaloulos, lygeros}@control.ee.ethz.ch

¹By the term conflict we define a situation where two aircraft violate required minimum separation standards, i.e. 5 nautical miles on the horizontal plane.

B. Model of the Vehicles

The problem under consideration involves N aircraft-like vehicles flying inside a planar circular workspace of radius r_{world} , while avoiding collisions with each other. Each aircraft $i = 1, \dots, N$ is modeled as a planar nonholonomic circular unicycle of radius r_i . The position and orientation of vehicle i are $\mathbf{q}_i = [x_i, y_i]^T$ and θ_i respectively. The motion of each vehicle is described by the following kinematic equations:

$$\dot{\mathbf{q}}_i = \begin{bmatrix} u_i \cos \theta_i \\ u_i \sin \theta_i \end{bmatrix} \quad (1a)$$

$$\dot{\theta}_i = \omega_i \quad (1b)$$

where u_i is the longitudinal (linear) and ω_i the angular velocity of vehicle i . The state of each vehicle is then $\mathbf{n}_i = [\mathbf{q}_i^T, \theta_i]^T$ while its input is $\mathbf{v}_i = [u_i, \omega_i]^T$. The vector of the positions of all vehicles is $\mathbf{Q} = [\mathbf{q}_1^T, \dots, \mathbf{q}_N^T]^T$.

The choice of the unicycle model for the aircraft is considered adequate for the motion planning task that we consider in this paper. It is assumed that a lower level control, like the Flight Management System (FMS) will be onboard to realize the trajectories provided by the proposed control scheme.

C. CD&R using Navigation Functions

Navigation functions in their original form are not suitable for the control of non-holonomic, aircraft-like vehicles, as they do not take into account the kinematic constraints of such vehicles. Application of the original NF method as introduced by Koditschek and Rimon [1] with a feedback law for the control of a nonholonomic vehicle can lead to undesired behavior, like having the vehicle rotate in place [4], [12]. In order to overcome this difficulty *Dipolar Navigation Functions* have been developed [12] which offer a significant advantage: the integral lines of the resulting potential field are all tangent to the desired orientation at the goal, eliminating in most cases the need for in-place rotation at the destination, as the vehicle is driven there with the desired orientation. This is achieved by using the plane whose normal vector is parallel to the desired orientation and includes the origin as an additional artificial obstacle.

The NF used in this paper is:

$$\Phi_i = \Phi_i(\mathbf{q}_i) = \frac{\gamma_{di} + f_i}{((\gamma_{di} + f_i)^k + H_{nhi} \cdot G_i \cdot \beta_{0i})^{1/k}} \cdot (2)$$

The above Navigation Function is constructed as explained in detail in [13]. The function $G_i = G_i(\mathbf{Q})$ reflects the proximity to any possible collisions involving vehicle i : G_i is zero when vehicle i participates in a conflict, i.e. when the sphere occupied by agent i intersects with other agents' spheres, and takes positive values away from any conflicts, while $\gamma_{di} = \gamma_{di}(\mathbf{q}_i) = \|\mathbf{q}_i - \mathbf{q}_{id}\|^2$ is the distance from the destination position \mathbf{q}_{id} . The function $f_i = f_i(G_i)$ is necessary in a decentralized approach as it is used in proximity situations in order to ensure that Φ_i attains positive values even when agent i has reached its destination. Thus

agent i can be temporarily driven away from its destination in order to facilitate the convergence of neighboring agents. As the workspace is considered spherical with radius r_{world} , the workspace bounding obstacle is $\beta_{0i} = r_{world}^2 - \|\mathbf{q}_i\|^2 - r_i^2$.

The factor H_{nhi} renders the potential field dipolar. It is responsible for the repulsive potential created by the artificial obstacle used to align the trajectories at the origin with the desired orientation θ_{di} :

$$H_{nhi} = \epsilon_{nh} + n_{nhi} \quad (3)$$

$$n_{nhi} = ([\cos \theta_i \quad \sin \theta_i] \cdot (\mathbf{q}_i - \mathbf{q}_{id}))^2 \quad (4)$$

where ϵ_{nh} is a small positive constant. Finally, k is a positive tuning parameter for this class of Navigation Functions.

The potential field function given above has been used in [5] and has proven navigation properties, i.e. it provides global convergence to the destination along with guaranteed collision avoidance. To better demonstrate this dipolar property, a simple potential field generated by such an NF, without any obstacles is presented in Figure 1. It can be seen that the surface $x = 0$ divides the workspace of radius $r_{world} = 100$ in two parts, and forces all the integral lines to approach the target $(0, 0)$ parallel to the y axis.

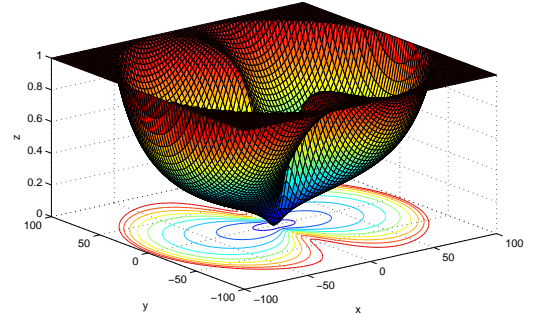


Fig. 1. Potential Field generated by a Dipolar Navigation Function

Each vehicle i is governed by the following control law [14]:

$$u_i = -\text{sgn}(P_i) \cdot F_i - \left(\frac{\partial \Phi_i}{\partial t} + \left| \frac{\partial \Phi_i}{\partial t} \right| \right) \frac{1}{2P_i} \quad (5a)$$

$$\omega_i = -k_{\theta_i} (\theta_i - \theta_{nhi}) + \dot{\theta}_{nhi} \quad (5b)$$

where

$$F_i = k_u \cdot \|\nabla_i \Phi_i\|^2 + k_z \cdot \|\mathbf{q}_i - \mathbf{q}_{id}\|^2$$

$$P_i = \mathbf{J}_{I_i}^T \cdot \nabla_i \Phi_i$$

$$\mathbf{J}_{I_i} = \mathbf{J}_{I_i}(\theta_i) = [\cos \theta_i \quad \sin \theta_i]^T$$

$$\nabla_i \Phi_j = \frac{\partial \Phi_j}{\partial \mathbf{q}_i}$$

$$\frac{\partial \Phi_i}{\partial t} = \sum_{j \neq i} u_j \nabla_j \Phi_i^T \cdot \mathbf{J}_{I_j}$$

MPC initialization:

Set $t = 0$
 initialize $\mathbf{X}(t)$

repeat:**initialization:**

Set $k = 0$
 Generate $\Theta_0 = \{\Theta(t), \dots, \Theta(t + (N - 1)T)\} \sim g(\Theta)$
 Calculate $(\mathbf{X}(t + (i - 1)T + 1), \dots, \mathbf{X}(t + iT)) =$
 $= O(\mathbf{X}(t + (i - 1)T), \Theta(t + (i - 1)T))$
 (recursively $\forall i \in \{1, \dots, N\}$)
 Set $C_0 = L(\mathbf{X}(t + 1), \dots, \mathbf{X}(t + NT))$

repeat:

Set $k = k + 1$
 Generate $\tilde{\Theta} = \{\tilde{\Theta}(t), \dots, \tilde{\Theta}(t + (N - 1)T)\} \sim g(\Theta)$
 Calculate $(\tilde{\mathbf{X}}(t + (i - 1)T + 1), \dots, \tilde{\mathbf{X}}(t + iT)) =$
 $= O(\tilde{\mathbf{X}}(t + (i - 1)T), \tilde{\Theta}(t + (i - 1)T))$
 (recursively $\forall i \in \{1, \dots, N\}$)
 Set $\tilde{C} = L(\tilde{\mathbf{X}}(t + 1), \dots, \tilde{\mathbf{X}}(t + NT))$
 Set $\rho_k = \min \left\{ \frac{C_{k-1}}{g(\Theta_{k-1})} \frac{g(\tilde{\Theta})}{\tilde{C}}, 1 \right\}$
 Set $[\Theta_k, C_k] = \begin{cases} [\tilde{\Theta}, \tilde{C}] & \text{with probability } \rho_k \\ [\Theta_{k-1}, C_{k-1}] & \text{with probability } 1 - \rho_k \end{cases}$

until $k = \text{maxsteps}$

Find $j : C_j = \min\{C_1, \dots, C_{\text{maxsteps}}\}$
 Calculate $\mathbf{X}(t + T) = O(\mathbf{X}(t), \Theta(t))$
 Set $t = t + T$

until $|(x_i(t), y_i(t)) - (x_i^{\text{final}}, y_i^{\text{final}})| < \Delta$

TABLE I

MPC USING RANDOMIZED OPTIMIZATION ALGORITHM

and k_u, k_z, k_{ϕ_i} are positive real gains. The angle $\theta_{\text{nh}i}$ is the angle of the gradient $\nabla \Phi_i$:

$$\theta_{\text{nh}i} \triangleq \begin{cases} \text{atan2}(\text{sgn}(p_i) \cdot \Phi_{iy}, \text{sgn}(p_i) \cdot \Phi_{ix}), & \mathbf{q}_i \neq \mathbf{q}_{id} \\ \theta_{id}, & \mathbf{q}_i = \mathbf{q}_{id} \end{cases}$$

where $\Phi_{ix} = \frac{\partial \Phi_i}{\partial x_i}$, $\Phi_{iy} = \frac{\partial \Phi_i}{\partial y_i}$ and $p_i = \mathbf{J}_{Iid}^T \cdot (\mathbf{q}_i - \mathbf{q}_{id})$, $\mathbf{J}_{Iid} = \mathbf{J}_I(\theta_{id})$ is the current position vector with respect to the destination, projected on the longitudinal axis of the desired orientation. Consequently $\text{sgn}(p_i)$ is equal to 1 in front of the target configuration and -1 behind it. Finally we define:

$$\text{sgn}(x) \triangleq \begin{cases} 1, & \text{if } x \geq 0 \\ -1, & \text{if } x < 0 \end{cases}$$

$$\text{atan2}(y, x) \triangleq \arg(x, y), \quad (x, y) \in \mathbb{C}.$$

The insight behind the above control law is to align the vehicle's longitudinal axis with the gradient of the potential field and drive the vehicle along an integral line to approach the destination with the desired orientation.

D. Stability Analysis

As shown in [14], each vehicle i described by the model (1) under the control law (5) is asymptotically stabilized to its target $\mathbf{q}_{id}, \theta_{id}$.

III. MODEL PREDICTIVE CONTROL FORMULATION

One important drawback of the use of NFs is that they cannot guarantee any constraint satisfaction on the trajectory. In our case, this can result in agents having to stop, travel in circles for some time, etc. While this is not a problem

in robotics, or even ground vehicle control, where the agents can stop and start again, the situation is different for aircraft, since physical and aerodynamic reasons impose constraints on the minimum and maximum speed, thrust, turning radius, etc.

To overcome this problem we employ the technique of Model Predictive Control (MPC) [8], a control methodology developed specifically to deal with state and input constraints. Denoting by T the periodicity of the controller and by N the length of the horizon of MPC, at each time step t , an optimization problem of horizon NT will be solved to find the optimal inputs for the NF. In an ATC setting, the Mid Term CR algorithm, which is centralized, does not have very detailed information on the dynamics and all the uncertainties involved. It is just responsible for transmitting to the aircraft any changes of their flight plan for avoiding potential conflicts. Thus, the MPC algorithm will view the NFs as a black box, which will produce state trajectories for all aircraft given their target destinations.

The state of each aircraft i at time t (as considered by the MPC algorithm) is $X_i(t) = [x_i(t), y_i(t), \theta_i(t), u_i(t), \omega_i(t)]^T$. Note that this notation makes no implication on the non-holonomic kinematic model (where $u_i(t), \omega_i(t)$ are outputs of the system) but represents the ignorance of the MPC on the details of the underlying model. The inputs of the NF are the intermediate destinations of the aircraft $\Theta_i(t) = [x_i^{\text{interm}}(t), y_i^{\text{interm}}(t)]$. For ease of notation, we introduce the variables $\mathbf{X}(t) = [X_1(t), \dots, X_n(t)]$ and $\Theta = [\Theta_1(t), \dots, \Theta_n(t)]$, where n denotes the number of aircraft. The NF is then viewed as an oracle $O(\mathbf{X}(t), \Theta(t))$ that, given the current aircraft state and the intermediate destinations, returns the state trajectory for the next T steps $(\mathbf{X}(t + 1), \dots, \mathbf{X}(t + T))$. The state evolution in the NFs can be influenced by uncertainty (in our case the wind speed). The MPC algorithm will try to minimize some cost function $L(\mathbf{X}(t + 1), \dots, \mathbf{X}(t + NT)) \in \mathbb{R}$, subject to constraints $\mathbf{X}(\tau) \in \mathbb{X}, \forall \tau \in \{t, t + T, \dots, t + NT\}$. The cost function reflects some long-term goals for the aircraft (e.g. reach their final destination as fast as possible, avoid turning too often, etc.). The constraints reflect operational constraints of the aircraft.

The finite horizon optimization problem described to be solved at each time t is a non-convex problem. Thus, the problem of finding the exact optimal value is computationally intractable. To overcome this difficulty we use randomized optimization algorithms. Randomized optimization algorithms are a very promising method in this context, since they can inherently deal with the complexity of the problem, with reasonable computational workload. There are several methods falling into this category, such as genetic algorithms [15], simulated annealing [16], etc. While all seem to work with more or less the same efficiency, only few provide guarantees for convergence to the optimum. This is the reason that we chose the method described in [17]. This method is a variation of simulated annealing based on Markov Chain Monte Carlo (MCMC) that works both for

deterministic and expected value criteria.

Of course, since our control has a receding horizon policy, at every time t , the optimal inputs for the time instants $t, t+T, \dots, t+(N-1)T$ will be calculated, but only the first will be applied. Then the control law will be recalculated at time $t+T$ for the time instants $t+T, \dots, t+NT$, etc. Due to uncertainties and conflict resolution maneuvers, aircraft might not arrive at their exact final destination, thus we will consider that aircraft reach their destination when the Euclidean distance between their current position and their final is less than some tolerance value Δ .

Our algorithm is summarized in Table I. Note that the proposal distribution from which random samples are extracted is very important for the algorithm to approximate the optimum inputs. Also important to note is that the dimension of the search space grows linearly in the prediction horizon N , which makes the optimization problem harder to solve for long prediction horizons. The proposed combination of MPC and NFs retains the safety guarantees (as at all times the NF potential field is repulsive with respect to neighboring aircraft), while handling constraints and cost factors through the optimization performed by MPC.

IV. SIMULATION SETTING AND RESULTS

A. Simulation Setting

In our simulation setting, we consider several aircraft in level flight converging to the same point (0,0) that have to be deconflicted. A typical configuration is presented in Figure 2 for three aircraft.

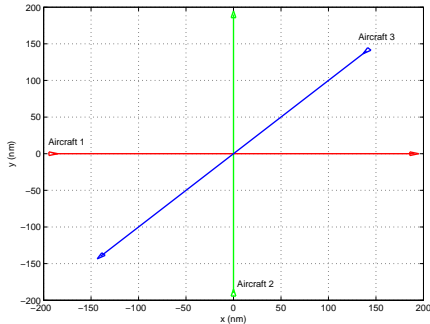


Fig. 2. Configuration for 3 aircraft encounter.

For all our simulations, we will assume that the aircraft are of type Airbus A321, flying at 33000ft, a typical cruising altitude for commercial flights. [18] suggests that the airspeed at this altitude can only vary in the region $[366, 540]$ knots, with a nominal value of 454 knots. We will enforce these constraints on our controller.

Regarding the uncertainty, we will only consider the wind speed as source of uncertainty. Wind speed (in general) can be modeled as a sum of two components: a nominal, deterministic component (available through meteorological forecasts) and a stochastic component, representing deviations from the nominal. Since the forecasts are available prior to the flights, flight plans are calculated taking them into account, so for simplicity reasons, we set the forecasted wind speed equal to zero. The stochastic part of the wind will

be generated by a Gaussian distribution with zero mean and standard deviation $\sigma = 5.17\text{m/s}$ [19]. Its strong correlation structure [20] implies that it cannot be represented as white noise; instead it is more accurate to approximate it by a constant random value for each simulation.

B. Control using Navigation Functions

First, we try to use the NFs method to deconflict this situation, in the case where uncertainty is set to zero, without applying MPC. Indeed, NFs manage to resolve the situation, with the aircraft converging to their destinations, without any conflicts arising. Their inability to respect system's constraints is, however, obvious, as indicated in Figure 3. The aircraft have a speed that is constantly decreasing and converges asymptotically to zero, as the aircraft approach their destination.

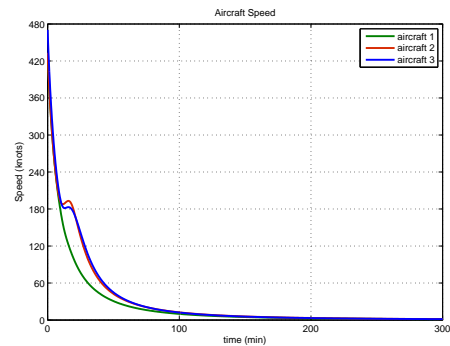


Fig. 3. Aircraft speed for the solution produced by NFs

This problem is inherent in Navigation Functions, since the speed of the agents heavily depends on the distance to their final destination. The situation becomes even worse when uncertainty is introduced. Since the trajectories of the aircraft depend only on the geometry of the situation in a deterministic manner, the only way for the NFs to correct the deviation because of the wind is to command different control inputs. The problem is that since the uncertainty is applied on the output trajectory, the solution converges to a different point, where the speed commanded by the NFs added to the wind speed equal zero. Thus, depending on the wind speed and its direction, some aircraft may never reach their destination.

C. MPC with NFs

As already discussed, the search space for the randomized optimization algorithm grows with the prediction horizon. On the other hand, we are interested in a fast implementation, if the control scheme is to be applied in ATC. To reduce the computational workload, one can do several things, like shortening the horizon, or calculating only one input for all times $\{t, t+T, \dots, t+(N-1)T\}$. The first would clearly reduce the advantage of the MPC approach, causing the system to enter states where no feasible solutions are available, while the second approach would introduce much conservatism in the controller.

To reduce conservatism on the second approach, we introduce a strategy for the optimization algorithm, where only

the input for time t will be optimized. Then, at time $t + T$, the new input (intermediate way point) for the predictive controller will be the same as that of time t , adding the distance covered by each aircraft, etc. until the input for time $t + (N - 1)T$. In this fashion, the controller will have taken into account the uncertainty encountered by the aircraft and will constantly try to keep the target at a constant distance, forcing the NFs to command airspeeds close in the desired range.

Exploiting the structure of the problem, it can be observed that a distance to the target around 100nm produces a speed for the aircraft matching the nominal cruising speed for our altitude. Thus, the search space will concentrate around points with a distance close to this value. This is done by sampling from a Gaussian with mean 100nm and standard deviation 10nm. Then, the intermediate waypoint is determined by uniformly sampling for an angle in $[-\frac{\pi}{2}, \frac{\pi}{2}]$ around the line segment joining the current position of the aircraft and its final destination.

D. Results

One can optimize over several costs in the optimization problem over several horizons and discretization steps. We chose $T = 5$ minutes, $N = 4$ and a cost function that tries to minimize the sum of the remaining distance to final destination at the end of the horizon for all aircraft:

$$L = \sum_i D(i, t + NT). \quad (6)$$

To evaluate the performance of our algorithm, we simulate each encounter using 1000 Monte Carlo runs. The randomized optimization algorithm will optimize at each time step over 1000 random extractions from the search space.

1) *4 aircraft encounter*: As a first example we will consider a situation where 4 aircraft are following paths that are converging at the same point. Using all the settings mentioned before, our control scheme resolves the situation in all 1000 runs, while respecting the speed constraints we impose on the aircraft airspeed (i.e. speed remains within [366, 540] knots). Figure 4 shows the mean speed (over all 1000 Monte Carlo runs), as well as the highest and lowest airspeeds observed for every aircraft at all times. The bounds on the speed are also drawn for convenience. The average running time for each simulation is 200 sec in a dual-core Pentium 3.2GHz, while the peak memory usage is around 110MB RAM. This time is many times faster than real time (which would be 66 min for this situation).

One can observe that the speed of the aircraft is very well regulated, with a mean value very close to the desired nominal airspeed for this altitude. Another interesting aspect is the minimum separation between all aircraft flying in the airspace. Simulating the situation with the NFs (without the MPC approach) for the deterministic case leads to a minimum separation of 22 nm. This is obviously quite conservative, since conflicts only happen when this separation drops below 5 nm. Our approach shows some major improvement in this aspect, resulting in minimum separations between

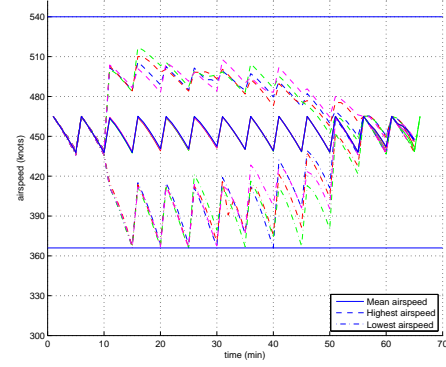


Fig. 4. Speed evolution with time for a conflicting situation of 4 aircraft

11.5 and 16 nm in all simulations. Thus, despite the presence of uncertainty, the aircraft can fly closer to one another, while comfortably respecting the safety separation criteria. The solution generated by the algorithm for a particular wind speed is shown in Figure 6, while NFs generate the trajectories shown in Figure 5 for the case where wind is not present.

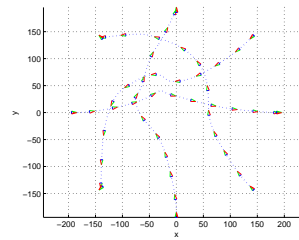


Fig. 5. Solution of NFs for a conflicting situation of 4 aircraft

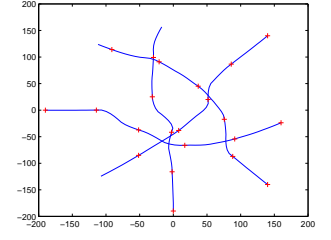


Fig. 6. Solution of the proposed scheme for a conflicting situation of 4 aircraft

2) *6 aircraft encounter*: We try to present the algorithm with an even more challenging problem: a situation where 6 aircraft are converging to the same point. Applying the same configuration for the NFs approach (for the deterministic case again), the trajectories one would get are shown in Figure 7. The solution demands all aircraft to travel in a circle of radius around 190 nm until they reach their destinations. Once again, the constraints are violated very often and the distance traveled to reach the goal is much larger than direct routing.

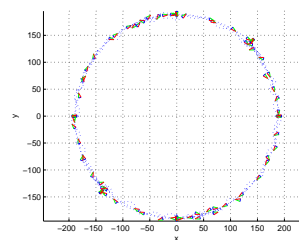


Fig. 7. Solution of NFs for a conflicting situation of 6 aircraft

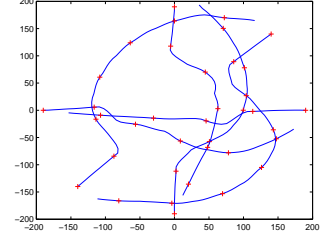


Fig. 8. Solution of the proposed scheme for a conflicting situation of 6 aircraft

The MPC approach can include the uncertainty modeling and once again can resolve the situation without problems. We present the mean speed (over all 1000 Monte Carlo runs),

as well as the highest and lowest airspeeds observed for every aircraft at all times in Figure 9. The speed for all aircraft is again very well regulated, having a mean value very close to the one desired at this altitude. The average running time in this case is around 1500 sec in the same PC, while the peak memory usage is around 130MB RAM. The higher computation time needed comes as no surprise, since the feasible solutions for the search space are much fewer in this case. One should note though, that the time needed is still more than 3 times faster than real flight time (which would be 85 min for this situation).

The solution generated by the algorithm for a particular extraction of the wind speed is shown in Figure 8. Aircraft now can travel smaller distances, while conflict avoidance and speed constraints are respected. This conservativeness reduction can help ATC to increase the capacity of the airspace, as the proposed scheme can handle much more complex situations.

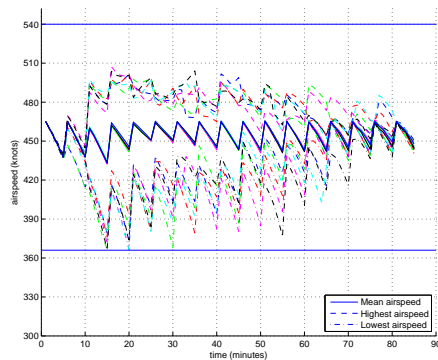


Fig. 9. Speed evolution with time for a conflicting situation of 6 aircraft

V. CONCLUSIONS AND FUTURE WORK

A novel control scheme combining the methods of Navigation Functions and Model Predictive Control has been presented. This control scheme exploits the ability of Model Predictive Control to handle constraints, while preserving the collision avoidance properties of Navigation Functions. We applied this approach to an Air Traffic Control problem, where uncertainty plays a great role in the system evolution and safety, while physical constraints have to be respected. The proposed scheme outperforms the existing Navigation Functions methods, respecting the system constraints, while reducing conservatism and optimizing over a desired cost for the system. Simulation results suggest that the method is robust under wind uncertainties.

Possible directions for future work include embedding more sources of uncertainty in the system (like radar measurement errors) and using the inputs for the Flight Management System of the aircraft in a more realistic Air Traffic Control simulator. Finally, it would be of interest to investigate whether using the analytic form of Navigation Functions for the MPC approach (instead of assuming black-box optimization) could lead to computationally tractable problems and theoretical guarantees on the convergence of the overall scheme.

VI. ACKNOWLEDGEMENTS

This research is supported by the European Commission under the project iFly, FP6-TREN-037180.

REFERENCES

- [1] E. Rimon and D. E. Koditschek, "Exact robot navigation using artificial potential functions," *IEEE Transactions on Robotics and Automation*, vol. 8, no. 5, pp. 501–508, 1992.
- [2] K. Loizou, S.G.; Kyriakopoulos, "Closed loop navigation for multiple holonomic vehicles," *Intelligent Robots and System, 2002. IEEE/RSJ International Conference on*, vol. 3, pp. 2861–2866 vol.3, 2002.
- [3] H. Tanner and A. Kumar, "Towards decentralization of multi-robot navigation functions," *Robotics and Automation, 2005. ICRA 2005. Proceedings of the 2005 IEEE International Conference on*, pp. 4132–4137, 18–22 April 2005.
- [4] H. G. Tanner and K. J. Kyriakopoulos, "Nonholonomic motion planning for mobile manipulators," *Proceedings of the 2000 IEEE International Conference on Robotics & Automation*, pp. 1233–1238, 2000.
- [5] D. V. Dimarogonas and K. J. Kyriakopoulos, "A feedback control scheme for multiple independent dynamic non-point agents," *International Journal of Control*, vol. 79, no. 12, pp. 1613–1623, 2006.
- [6] H. G. Tanner and A. Kumar, "Formation stabilization of multiple agents using decentralized navigation functions," in *Proceedings of Robotics: Science and Systems*, Cambridge, USA, June 2005.
- [7] G. P. Roussos, D. V. Dimarogonas, and K. J. Kyriakopoulos, "3d navigation and collision avoidance for a non-holonomic vehicle," *2008 American Control Conference, Seattle, Washington, USA, 2008*.
- [8] J. Maciejowski, *Predictive Control with Constraints*. Prentice Hall, 2001.
- [9] K. Dimarogonas, D.V.; Kyriakopoulos, "Decentralized stabilization and collision avoidance of multiple air vehicles with limited sensing capabilities," *American Control Conference, 2005. Proceedings of the 2005*, pp. 4667–4672 vol. 7, 8–10 June 2005.
- [10] J. Kuchar and L. Yang, "A review of conflict detection and resolution methods," *IEEE Transactions on Intelligent Transportation Systems*, vol. 1, no. 4, pp. 179–189, 2000.
- [11] D. E. Koditschek and E. Rimon, "Robot navigation functions on manifolds with boundary," *Adv. Appl. Math.*, vol. 11, no. 4, pp. 412–442, 1990.
- [12] H. G. Tanner, S. Loizou, and K. J. Kyriakopoulos, "Nonholonomic navigation and control of cooperating mobile manipulators," *IEEE Transactions on Robotics and Automation*, vol. 19, no. 1, pp. 53–64, 2003.
- [13] D. V. Dimarogonas, S. G. Loizou, K. J. Kyriakopoulos, and M. M. Zavlanos, "A feedback stabilization and collision avoidance scheme for multiple independent non-point agents," *Automatica*, vol. 42, no. 2, pp. 229–243, 2006.
- [14] G. P. Roussos, D. V. Dimarogonas, and K. J. Kyriakopoulos, "Decentralized 3d navigation and collision avoidance for multiple nonholonomic agents," *European Control Conference, 2009*, submitted.
- [15] J. Holland, *Adaptation in Natural and Artificial Systems: An Introductory Analysis With Applications to Biology, Control, and Artificial Intelligence*. MIT Press, 1992.
- [16] S. Kirkpatrick, C. D. Gelatt, and M. P. Vecchi, "Optimization by simulated annealing," *Science, Number 4598, 13 May 1983*, vol. 220, 4598, pp. 671–680, 1983. [Online]. Available: citeseer.ist.psu.edu/kirkpatrick83optimization.html
- [17] A. Lecchini-Visintini, J. Lygeros, and J. Maciejowski, "Simulated annealing: Rigorous finite-time guarantees for optimization on continuous domains," *Advances in Neural Information Processing Systems*, vol. 20, 2007.
- [18] Eurocontrol Experimental Centre, *User Manual for the Base of Aircraft Data (BADA)*, 2004. [Online]. Available: <http://www.eurocontrol.fr/projects/bada/>
- [19] B. Schwartz, S. Benjamin, S. Green, and M. Jardin, "Accuracy of RUC-1 and RUC-2 wind and aircraft trajectory forecasts by comparison with ACARS observations," *Weather and Forecasting*, vol. 15, no. 3, pp. 316–326, 2000.
- [20] G. Chaloulos and J. Lygeros, "Effect of wind correlation on aircraft conflict probability," *AIAA Journal of Guidance, Control and Dynamics*, vol. 30, no. 6, pp. 1742–1752, 2007.